Marine Chemistry 204 (2018) 36–48

Contents lists available at ScienceDirect

Marine Chemistry

journal homepage: www.elsevier.com/locate/marchem

Copper-binding ligands in the NE Pacific

Hannah Whitby[a,*], Anna M. Posacka[b], Maria T. Maldonado[b], Constant M.G. van den Berg[c]

[a] LEMAR, Technopole Brest Iroise, Plouzané F29280, France
[b] University of British Columbia, BC V6T 1Z4, Vancouver, Canada
[c] University of Liverpool, L69 3GP Liverpool, UK

ARTICLE INFO

Keywords:
Copper speciation
Seawater
Thiols
Humic substances
Cathodic stripping voltammetry
Thiourea
Glutathione
Organic ligands

ABSTRACT

Copper distribution and speciation were determined at stations P4 and P26 along Line P as part of a GEOTRACES Process Study in the Northeast Pacific, at depths between 10 and 1400 m. Two ligand classes (L_1 and L_2) were detected at both stations: the stronger L_1 ligand pool with log K'_{Cu2+L1} 15.0–16.5 and the weaker L_2 ligand pool with log K'_{Cu2+L2} 11.6–13.6. The L_1 class bound on average 94% of dCu, with the ratio between L_1 and dCu constant and close to unity (1.15 = $[L_1]$:[dCu]). The concentrations of total ligands exceeded those of dCu at all depths, buffering Cu^{2+} concentrations ($[Cu^{2+}]$) to femtomolar levels (i.e. pCu 14.1–15.7). Measurements using cathodic stripping voltammetry also identified natural copper-responsive peaks, which were attributed to thiourea- and glutathione-like thiols (TU and GSH, respectively), and Cu-binding humic substances (HS_{Cu}). Concentrations of TU, GSH and HS_{Cu} were determined by standard addition of model compounds in an attempt to identify Cu-binding ligands. HS_{Cu} concentrations were generally higher at P26 than at P4, consistent with a marine origin of the humic material. Overall, HS_{Cu} contributed to 1–27% of the total L concentration (L_T) and when combined with the two thiols contributed to up to 32% of L_T. This suggests other ligand types are responsible for the majority of dCu complexation in these waters, such as other thiols. Some potential candidates for detected, but unidentified, thiols are cysteine, 3-mercaptopropionic acid and 2-mercaptoethanol, all of which bind Cu. Significant correlation between the concentrations of TU-like thiols and L_1, along with the high log K'_{Cu2+L1} values, tentatively suggest that the electrochemical TU-type peak could be part of a larger, unidentified, high-affinity Cu compound, such as a methanobactin or porphyrin, with a stronger binding capability than typical thiols. This could imply that chalkophores may play a greater role in oceanic dCu complexation than previously considered.

1. Introduction

Complexation by natural organic ligands (L) controls the speciation of biogenic metals in seawater (Bruland et al., 2014). Approximately 99% of total dissolved copper (dCu) exists as relatively stable, organic complexes throughout the water column (Buck et al., 2007; Moffett and Dupont, 2007). Organically bound Cu is less bioavailable, and thus less toxic, than free Cu^{2+}. Indeed, free Cu^{2+} at pM levels can be toxic to cyanobacteria (Brand et al., 1986) but potentially growth-limiting to some archaea that have a greater Cu requirement (Amin et al., 2013). Cu tolerances and requirements vary among phytoplankton species and phylogenetic classes, as well as between coastal and oceanic strains of the same genus (Annett et al., 2008; Peers et al., 2005).

Cu complexation with natural organic ligands depends on the ligand concentrations and the complex stability (conditional stability constant, K'_{Cu2+L}). Log K'_{Cu2+L} values in the literature are typically subdivided into two classes (L_1 and L_2), with log K'_{Cu2+L1} around 13–16 and log K'_{Cu2+L2} around 10–13 (Buck and Bruland, 2005; Bundy et al., 2013; Moffett and Dupont, 2007; Muller and Batchelli, 2013). In addition to controlling bioavailability to marine microorganisms, organic complexation influences Cu distributions by reducing scavenging (Vance et al., 2008), a major Cu sink in the global ocean (Boyle et al., 1977). Metals are scavenged by suspended particulate matter (SPM) originating from suspended sediments, algal blooms and aerosols (Kies et al., 1996; Rivier et al., 2012; Rogan et al., 2016; Schleicher et al., 2010). As a result, Cu typically displays a hybrid between a scavenged and a nutrient-like profile in open ocean waters (Bruland et al., 2014; Jacquot and Moffett, 2015; Little et al., 2013).

Riverine inputs are the dominant source of Cu to the oceans (Bruland et al., 2014). In estuarine waters, terrestrially-derived humic substances (HS) account for a major fraction of the available organic ligands for Cu complexation (Abualhaija et al., 2015; Muller and Batchelli, 2013) and play a key role transporting metals, particularly iron (Fe) to coastal and open ocean waters (Bundy et al., 2015; Laglera

* Corresponding author.
E-mail address: hannah.whitby@univ-brest.fr (H. Whitby).

https://doi.org/10.1016/j.marchem.2018.05.008
Received 30 January 2018; Received in revised form 7 May 2018; Accepted 26 May 2018
Available online 31 May 2018

and van den Berg, 2009; Misumi et al., 2013). Terrestrial HS are derived from the relatively recent degradation of plant matter (Averett et al., 1994) and are highly aromatic (Ruggiero et al., 1979; Sohn and Weese, 1986), forming organic Cu complexes in seawater with log K'_{Cu2+L} = 12–13 (Kogut and Voelker, 2001; Whitby and van den Berg, 2015). Humic substances are also expected to be important in metal speciation in open ocean waters (Heller et al., 2013; Kitayama et al., 2009), given that 5–25% of dissolved organic carbon (DOC) in the surface ocean is HS (Benner, 2002). But, in contrast to terrestrial HS, marine-derived HS are highly aliphatic (Sohn and Weese, 1986), with higher protein and carbohydrate content (Ertel and Hedges, 1983). Potential sources of marine HS may include marine bacteria (Romera-Castillo et al., 2011; Shimotori et al., 2009), decaying phytoplankton such as diatoms (Lorenzo et al., 2007) and the crosslinking of fatty acids released from the biota into oxygenated, sunlit seawater—a process known as humification (Harvey et al., 1983; Kieber et al., 1997). Though significant chemical differences exist between terrestrial and marine HS, their behaviour as Fe and Cu-binding ligands are remarkably similar, as their complexing sites are consistent (Sohn and Weese, 1986). However, despite the suspected existence of marine humics, to date there are no Cu-binding humic profiles from the open ocean.

Various reduced sulphur substances (RSS), such as thiols and phytochelatins, may also be important in oceanic Cu complexation. Glutathione (GSH), cysteine (Cys), arginine-cysteine and glutamine-cysteine are a few examples of RSS released in response to Cu toxicity (Dupont and Ahner, 2005; Leal et al., 1999) and have all been measured in open ocean waters (Dupont et al., 2006; Swarr et al., 2016). The combined concentrations of certain thiols (thiourea- like, TU) and copper-binding humic substances (HS_{Cu}) have been found to correlate very well with the concentration of Cu-binding ligands measured in estuarine waters (Whitby et al., 2017), and sulphur-containing copper compounds with azole-like functional groups have been detected in ocean waters (Boiteau et al., 2016).

Fe is arguably the best studied trace metal due to its role as a limiting nutrient for primary productivity in up to 40% of the ocean (Boyd, 2007; Moore et al., 2013), in regions described as high nutrient, low chlorophyll (HNLC). In response to Fe deficiency, some organisms have evolved mechanisms to reduce their Fe requirements or increase their efficiency at acquiring Fe, with some of these mechanisms relying on the availability of Cu (Maldonado et al., 2006; Peers and Price, 2006; Peers et al., 2005). Certain diatoms show growth co-limitation by Cu and Fe (Annett et al., 2008) while others exhibit higher Cu requirements when Fe-limited (Annett et al., 2008; Guo et al., 2012). *Pseudo-nitzschia*, a common pennate diatom after Fe enrichments in HNLC regions, has a low-Fe adaptive strategy, which relies on Cu and domoic acid (Maldonado et al., 2002; Wells et al., 2005). These examples demonstrate a physiological interaction between Cu and Fe, which could be in part due to the ability of Cu and Fe to form complexes with mutual ligands, such as domoic acid (Rue and Bruland, 2001) and humic substances (Kitayama et al., 2009; Kogut and Voelker, 2001). Thus, competition between these metals for humic-type ligands (Abualhaija et al., 2015; Yang and van den Berg, 2009) or for other organic complexes may occur, suggesting that the biogeochemical cycles of Cu and Fe may be interlinked.

Extending ~1500 km off the coast of Vancouver Island in the subarctic NE Pacific, Line P is comprised of 26 stations, with station P26 at 50°N 145°W in the HNLC region of the Alaskan gyre (Fig. 1). Indeed, in this region utilisation of macronutrients by phytoplankton communities is hindered by a lack of Fe, particularly after P20, establishing a gradient in HNLC conditions along the transect (Martin and Fitzwater, 1988; Schuback et al., 2015; Semeniuk et al., 2016b). Experiments in these and other HNLC waters have demonstrated that Fe addition stimulates phytoplankton blooms (de Baar et al., 2005). Although Fe is well studied in this region (Lam et al., 2006; Nishioka et al., 2001), less is known about the controls of Cu complexation. In this work we attempt to identify some of the ligands governing Cu speciation at two opposing sites along Line P. We measured the concentration of dCu and Cu-binding ligands at P4, a continental slope station and at P26, the most open ocean station, and compared them to measurements of the abundance of HS_{Cu} and suspected TU- and GSH-type thiols.

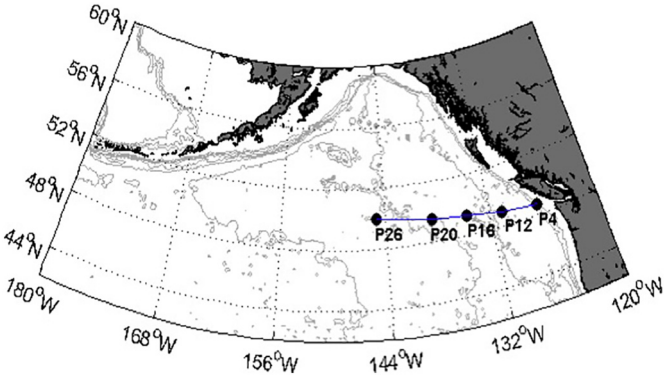

Fig. 1. A map of the NE Pacific, showing the Line P transect with the major stations, including stations P4 and P26 used in this study. Bathymetry was contoured at 1000 m intervals.

2. Materials and methods

2.1. Sample collection

Samples were collected from stations P4 and P26 of the Line P transect (Fig. 1, bottom depths 1317 m and 4226 m respectively) from 14 to 30 August 2012 (cruise 2012–13) on board the Canadian Coast Guard Ship John P. Tully. Sample bottles were cleaned according to GEOTRACES protocols (Buck et al., 2012; Cutter et al., 2010) and stored in MQ for at least a week after acid-cleaning. Samples for Cu speciation were collected into 12 L Teflon-coated GO-FLO (General Oceanics, FL USA) bottles attached to a 12-bottle powder-coated trace metal-clean rosette system modified according to Measures et al. (2008). The seawater was gravity-filtered from the GO-FLO bottles through 0.2 µm AcroPak filters (Pall Corporation) into 0.5 L fluorinated linear polyethylene (FLPE) bottles, and was immediately frozen at −20 °C until analysis. Before analysis, the seawater samples were thawed, swirled gently and left to come to room temperature (20 °C) in the dark. Samples were measured within 3 days of defrosting, and stored in the dark at 4 °C when not in use. Macronutrient and CTD data are courtesy of the Canadian Institute of Ocean Sciences, Department of Ocean & Fisheries, and are publically available (www.waterproperties.ca/linep/index.php, accessed 03/05/18).

2.2. Equipment and reagents

The voltammetric equipment used was a µ-Autolab III potentiostat (Ecochemie, Netherlands) connected to a 663 VA stand (Metrohm) with hanging mercury drop electrode (HMDE). The reference electrode was Ag/AgCl with a 3 M KCl salt bridge and a glassy carbon counter electrode. Solutions were stirred with a rotating polytetrafluoroethylene (PTFE) rod. Water used for rinsing and dilution of reagents was purified by reverse osmosis (Millipore) and deionisation (Milli-Q). Silica and PTFE voltammetric cells used for total Cu measurements were cleaned using 0.1 M HCl (trace metal grade) and rinsed with MQ water. The UV-digestion apparatus contained a high-pressure, 125-W mercury-vapour lamp (van den van den Berg, 2014) either positioned horizontally above a sample aliquot in a voltammetric cell, or surrounded by four 30-mL silica sample tubes with PTFE caps. Voltammetric scans used the square-wave mode for anodic stripping voltammetry (ASV) and differential-pulse mode for cathodic stripping voltammetry (CSV). Sample (10 mL) was purged with nitrogen for 5 min to remove dissolved oxygen

prior to analysis and mercury usage was minimised by modifying the software to discard 2, rather than 4, drops of mercury between scans.

Cu standards were prepared by dilution of an atomic absorption spectrometry standard solution (BDH SpectrosoL grade) in 0.01 M trace metal grade HCl. ASV was used to determine the concentration of dCu in some of the samples at pH 1.9 using trace metal grade HCl for acidification. CSV was used to determine the concentration of dCu and its chemical speciation at near-natural pH in the presence of 0.01 M borate/ammonia pH buffer, pH_{NBS} 8.15 (Campos and van den Berg, 1994). The stock borate/ammonia pH buffer (1 M boric acid/0.3 M ammonia) was UV-digested to remove organic matter; contaminating metals were removed by equilibration with 100 μM manganese dioxide (MnO_2) followed by filtration (van den Berg, 1982a).

2.3. Total dissolved copper

Concentrations of dCu at P26 were determined by CSV in the presence of 20 μM salicylaldoxime (SA) and 0.01 M borate/ammonia pH buffer (Campos and van den Berg, 1994). Prior to the CSV measurements, the sample was UV-irradiated at the original sample pH in conditioned silica tubes, or directly in a conditioned silica voltammetric cell, for 45 min (van den van den Berg, 2014) and left to cool before addition of reagents. The deposition potential (E_{dep}) was −0.15 V, the deposition time was 30 s scanning from E = 0 to −0.7 V in the differential pulse mode, with a 1-s potential jump to −1.2 V to desorb any residual organic matter from the electrode. The surface (10 m) and deep (1200 m and 1400 m) samples were also analysed by ASV at pH 1.9 (Allen et al., 1970) and also UV-oxidised, to allow for inter-comparison with reference seawater of that pH. Comparative measurements between CSV and ASV were found to give results within the standard deviation, and ASV measurements on NASS-6 reference material gave results within 5% of the certified value. All dCu samples from P4 were subsequently measured using ASV. These samples were UV-irradiated at pH 1.9 in acid-cleaned silica UV tubes, and measured at pH 1.9, E_{dep} of −0.9 V for 300 s, followed by 5 s at −1.4 V, scanning from E = −0.9 to −0.05 V in the differential pulse mode.

2.4. Humic substances

Cu-binding humic substances (HS_{Cu}) were determined by CSV in the presence of borate/ammonia pH buffer and excess Cu (30 nM) (Whitby and van den Berg, 2015). The method was modified to increase the limit of detection by using a longer deposition time of up to 5 min. Suwannee River humic acid (SRHA, International Humic Substances Society (IHSS) Standard II 2S101H) was used as reference humic acid, dissolved in MQ water to a stock concentration of 1 g L^{-1} and stored in the dark at 4 °C when not in use. Fresh dilutions of 0.01 g L^{-1} were prepared weekly. Concentrations of HS_{Cu} calibrated on the scale of μg HA L^{-1} were converted to the pM scale by multiplying with the binding capacity of 18.0 pmol Cu μg^{-1} HS_{Cu} (Whitby and van den Berg, 2015).

2.5. Thiols

A suspected thiol peak was observed in voltammetric scans of all samples, between −0.41 and −0.58 V. The peak was broad and sometimes asymmetrical, suggesting the presence of a mixture of different thiol types (Supplementary Table 1; Supplementary Fig. 1). Both glutathione (GSH) and thiourea (TU) increased the height of the broad thiol peak in the samples despite typically appearing at slightly different potentials in other work (Laglera and van den Berg, 2003), therefore both GSH and TU were selected as thiol standards. Although both GSH and TU bind Cu, voltammetric measurements of GSH and TU differ in that GSH is detected at the electrode as a Cu species with an optimum deposition potential of −0.2 V in the presence of excess Cu, whereas TU is measured as a mercury species (Hg-TU). Thus TU is measured without Cu addition, using a more positive deposition potential (+0.05 V) to maximise Hg- and minimise Cu-complexation (Laglera and Tovar-Sanchez, 2012; Whitby et al., 2017). Two types of thiol measurements were therefore performed on the thiol peak, by measuring the peak height with and without excess Cu with standard additions of GSH and TU, respectively.

Stock standard solutions were prepared by dissolving reagent grade GSH and TU (Fluka) in MQ to a concentration of 0.1 M and kept in the dark at 4 °C, with dilutions prepared to 10^{-6} M and 10^{-7} M. GSH and TU measurements were by CSV in the presence of borate/ammonia pH buffer. Thiourea concentrations (measured as Hg-TU) were determined without addition of Cu, with a deposition time of up to 5 min at E_{dep} = +0.05 V. The suspected TU thiol peak at P26 was sharper and slightly more negative than at P4, suggesting the dominance of TU-type thiols (Laglera and van den Berg, 2003). Therefore, TU concentrations in the P26 samples were calibrated by standard additions of TU to all samples. The limit of detection (LOD) was calculated from 3× the standard deviation of the standard addition calibration and was found to be around 15 pM. For P4 samples, the sensitivity (S, nA/nM) was calibrated by standard addition of TU to samples from depths of 10, 25, 50 and 75 m, giving values for S within 2% between the 4 samples. The average value of S was then used to calibrate the CSV of subsequent samples at P4, to obtain the TU concentration without further standard additions, minimising the risk of carry-over contamination.

At P4, the thiol peak was generally broader, less sharp and at a slightly more positive potential, better resembling a Cu-binding thiol such as GSH (Laglera and van den Berg, 2003). The deposition potential was either −0.2 V or +0.05 V for GSH, in the presence of Cu (30 nM) added in excess of the ligand concentrations. Although the sensitivity for GSH was greater at −0.2 V, the final concentration from standard additions was the same at both deposition potentials. GSH measurements were calibrated by standard additions to all samples from P4, except at 400, 600, 800 and 1200 m due to instability of the thiol peak across repeat measurements at these depths, potentially related to the presence of interfering substances in waters from the oxygen minimum zone (OMZ). At these depths, the calibrated S from measurements at other depths was used to calculate the concentration from the initial peak height (as for TU at P4). At P26, the sensitivity of the GSH-like Cu-thiol species was calibrated by standard additions of GSH in the 50 m sample and used to calculate the concentration from the peak height for samples from other depths.

2.6. Complexing capacity titrations

Concentrations of Cu-complexing ligands (L) in each sample were determined by titrations with Cu, using CSV and competitive ligand exchange (CLE-CSV) against SA to determine labile dCu in equilibrium conditions (Campos and van den Berg, 1994). For each titration, 170 mL seawater was poured into a 250-mL Teflon bottle (Nalgene), and 0.01 M borate/ammonia pH buffer and 10 μM SA (final concentrations) added. Aliquots of 10 mL of the seawater, buffer and SA mixture were pipetted into fourteen 25-mL polystyrene (Sterilin) vials with lid (polyethylene). Voltammetric cells used for titrations were rinsed with MQ followed by sample between titrations; the titration-vials were not rinsed to minimise de-conditioning of the vials. Cu was added to each vial in steps of progressively increasing concentration, typically from 0 nM to 12.5 nM. The usual Cu additions were 0, 0.25, 0.5, 0.75, 1, 1.5, 2, 2.5, 3, 4, 5, 7.5, 10, 12.5 nM Cu, with the remaining sample mixture in the bottle used for conditioning the cell and as additional initial (0 nM added Cu) points. The vials were left to equilibrate for a minimum of 8 h in the dark prior to analysis. The labile Cu concentration was determined by CLE-CSV using a 60 s deposition time at E_{dep} = −0.15 V. This was followed by a 9 s quiescence period at 0 V from where the scan was initiated, to −0.8 V. Two fresh Cu additions were made at the end of each titration (usually two additions of 2.5 or 5 nM) and measured immediately (i.e. not equilibrated) in order to

calibrate the sensitivity and ensure all ligands had been titrated, but were not used in the data fitting, except for P4 75 m and 100 m samples, which had high ligand concentrations exceeding the Cu additions of the titration.

Data were interpreted using the 'complete complexation fitting model' option in independent ProMCC software (Omanovic et al., 2015), and compared to Ruzic-van den Berg and Langmuir/Gerringa non-linear fitting methods within the same software (Gerringa et al., 1995; Ruzic, 1982; van den Berg, 1982b). Values from the different fitting methods typically compare very well; however, sometimes it is possible to obtain different fits even for a 14-point titration with relatively low noise. For example, Supplementary Fig. 6 shows a titration curve for sample P26, 50 m, where the following ranges were obtained for each parameter using the different fitting methods: L_1 = 2.1–2.6 nM, log K'_{Cu2+L1} = 15.3–15.5, L_2 = 3.8–4.8 nM, log K'_{Cu2+L2} = 13.0–13.6. Since each fitting method has limitations and to be inclusive of the error surrounding these measurements and fitting procedures, the data are presented are an average (± SD) of all of the values from each of the fitting methods described, with the error inclusive of the differences between fitting methods. Complex stabilities (log K'_{Cu2+L1} values) were calculated on the basis of Cu^{2+} and L′, as they are affected by side-reactions of the ligand (L) with major seawater cations and H^+, and are therefore conditional for experimental salinity and pH.

3. Results and discussion

3.1. Hydrography

The Eastern North Pacific has a growing, seasonally variable oxygen minimum zone (OMZ) at around 300–2000 m along the majority of the eastern boundary, with O_2 concentrations between 7 and 60 μM at the core (850–1080 m; Paulmier and Ruiz-Pino, 2009). During our study, dissolved oxygen concentrations were below 50 μM between 600 and 1800 m depth. In the summer along Line P, the euphotic zone ranges from ~20 to 50 m, and the mixed layer from 15 to 30 m (Semeniuk et al., 2016a). During this study, phytoplankton productivity was high in the surface at P4, with 5.7 μg *chla* L^{-1} at 6 m, decreasing to 0.1 μg *chla* L^{-1} by 31 m (www.waterproperties.ca/linep/index.php). In contrast, at P26 *chla* levels were much lower overall, with less variation with depth, decreasing from 0.62 μg *chla* L^{-1} at 6 m to 0.55 μg *chla* L^{-1} at 30 m. Below the euphotic zone, P4 is influenced by the warm and salty waters of the California Undercurrent (CUC, 150–200 m), and P26 by the fresher, cooler North Pacific Intermediate Waters (NPIW) (McAlister, 2015), strongest at around 200 m (Ueno and Yasuda, 2003).

3.2. Total dissolved copper

The trend in dCu concentration with depth in our 2012 samples is consistent with dCu values in samples taken in 2011, measured using flow injection, by chemiluminescence detection (Posacka et al., 2017). In general, the dCu concentrations were higher at the open ocean station, P26, than at the continental slope station, P4 (Fig. 2, Table 1). At P4 dCu concentrations ranged from 1.2 to 3.0 nM, with the highest concentrations at 10 m and 1200 m (Fig. 2A). At P26, dCu ranged from 2.1 to 3.3 nM, with lower concentrations in the upper 100 m (2.3 ± 0.1 nM, Fig. 2B).

The concentrations of dCu for both stations fall within the range of concentrations found in this region previously (Bruland, 1980; Coale and Bruland, 1988). The trend at each station is similar to the central North Pacific where dCu decreased from 3 nM to 1.5 nM in the upper thermocline, followed by an increase to 4–6 nM between 750 and 4000 m (Boyle et al., 1977), and to measurements from stations in the NW Pacific (~1–4 nM between 0 and 1500 m; (Moffett and Dupont, 2007). These values are higher than in the eastern tropical South Pacific where surface concentrations reached as low as 0.26 nM, the lowest dCu concentrations reported (Jacquot et al., 2013).

At the continental slope station, P4, the high dCu concentrations at 10 m (2.9 nM) have been suggested to be derived from fluvial rather than atmospheric inputs (McAlister, 2015; Posacka et al., 2017; Semeniuk et al., 2016a), while high dCu below 800 m (2.4–3.0 nM) is associated with diffusive Cu flux from the sediments (Posacka et al., 2017; Schallenberg et al., 2015). Cu concentrations remained below 2 nM between 75 and 800 m, with no input signal from the shelf (located at 1320 m depth), despite being a source of Fe to these depths in the northeast Pacific (Cullen et al., 2009).

At P26, dCu was between 2.1 and 2.4 nM in the upper 100 m. Upwelling of deep, dCu-rich waters of the Alaska gyre is a likely source of dCu to the upper waters at P26 (Posacka et al., 2017). In addition, temporal variability in dCu concentrations in the upper 300 m at P26 has been partly attributed to aerosol deposition from the west (Posacka et al., 2017). Below 200 m, dCu at P26 maintained a steady concentration with values (2.9–3.3 nM) generally higher than at P4, similar to zinc in this region (Janssen and Cullen, 2015). Correlations between macronutrients (phosphate and silicate) and dCu in the upper waters reveal shallow remineralisation, with decoupling below 300–400 m, coinciding with the upper boundary of the OMZ (Posacka et al., 2017).

Generally lower dCu concentrations at P4 than at P26 (averaging 1.9 vs. 2.7 nM, respectively, across the upper 1200 m) may seem surprising, given that P4 is a continental slope station and is expected to have higher coastal dCu loading. Elevated concentrations at P26 are likely due to upwelling, which also resulted in elevated dCu concentrations offshore the previous year (Posacka et al., 2017). Regular monitoring stations along the coast show that upwelling generally occurs in the summer months, with positive upwelling indices recorded nearby during the sampling timeframe (data from https://www.pfeg.noaa.gov/products/PFEL/modeled/indices/upwelling, accessed 03/05/2018). Furthermore, SPM is likely much higher at P4, from anthropogenic and natural inputs of particles from the coast, as well as local primary productivity. Higher SPM would potentially induce higher rates of scavenging, and indeed dCu at P4 exhibits a depth profile more typical of a scavenged than a nutrient-like element (Fig. 2A). Fluorescence data demonstrates that productivity was much higher in the surface waters of P4 (13 mg m^{-3}) than P26 (1.8 mg m^{-3}), decreasing dramatically down to 0.1 mg m^{-3} within the top 50 m at P4, and more steadily at P26 (0.8 mg m^{-3} at 50 m and 0.13 mg m^{-3} at 100 m). Low surface macronutrient concentrations are linked to the high fluorescence in the upper 30 m at P4 and may contribute to the sudden decrease in fluorescence with depth (fluorescence and macronutrient data available at www.waterproperties.ca/linep/index.php).

3.3. Copper speciation

The detection window of our CLE-CSV titrations was centred on $\alpha_{CuSA} = 1.3 \times 10^5$ (log α_{CuSA} = 5.1) using 10 μM SA. This SA concentration was selected to improve the sensitivity for the strong ligands (L_1 type), given that microorganisms in this region have been shown to access Cu bound to natural and artificial ligands with log K'_{Cu2+L} as high as 15.8 (Semeniuk et al., 2015). The titrations had sufficient resolution to also identify the weaker L_2-type ligands. We carried out experiments to verify whether the different ligand classes found here could be determined with 2 μM SA and found that the peaks used to fit L_1 were often below the detection limit, as demonstrated in titrations with multiple detection windows in Antarctic waters (Bundy et al., 2013).

At both stations, two ligand classes were detected (using 10 μM SA, Table 1) with ligand concentrations of 1–4 nM for L_1 and 1–20 nM for L_2 (Figs. 2A and B) and mean complex stabilities (log K'_{Cu2+L} values) of 15.6 ± 0.4 and 13.0 ± 0.4, respectively (Fig. 3A and B). These two distinct ligand classes were detected at all depths at both stations, except at P26 at 1400 m where only a single ligand class could be fitted, and at 600 m, which did not have adequate sample volume for a

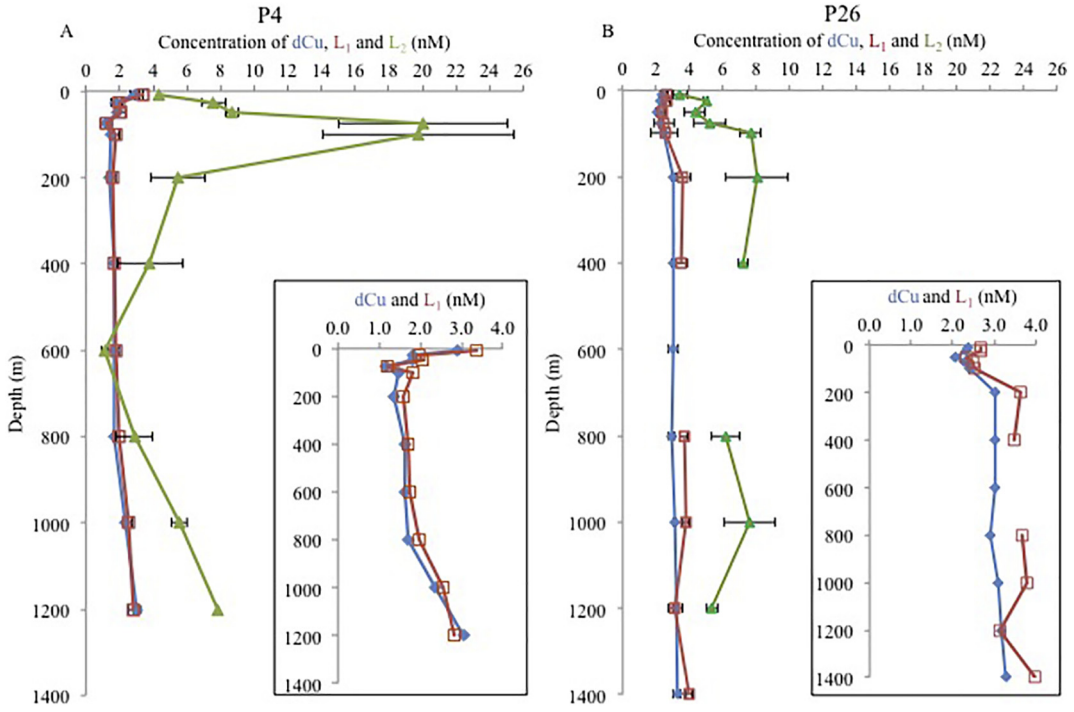

Fig. 2. Profiles of total dissolved copper (dCu) (blue), L_1 (red) and L_2 (green) for (a) station P4 and (b) station P26 in the NE Pacific, with inset plots of dCu and L_1 profiles for each station. Station depths: P4 1317 m, P26 4226 m. (For interpretation of the references to colour in this figure legend, the reader is referred to the web version of this article.)

titration.

The concentration of L_1 was either similar or slightly in excess of dCu in all samples, following a similar profile to that of dCu at both stations (Fig. 2B). The concentrations of L_1 were higher at P26 (2.3–4 nM) than at P4 (1.2–3.4 nM, Fig. 2, Table 1), mirroring the variation in dCu. The exception was the surface sample (10 m), which had higher L_1 concentration and dCu at P4 than P26 (3.4 vs. 2.7 nM). Mean log K'_{Cu2+L1} for L_1 was 15.8 ± 0.3 at P4 and 15.3 ± 0.2 at P26, which are typical of strong ligands (Bruland et al., 2000). Although concentrations of dCu and L_1 were lower at P4 than at P26, interestingly, log K'_{Cu2+L1} were slightly higher at P4 than at P26 in the upper waters (10–200 m), but similar at depths deeper than 200 m (Fig. 3A and B). The correlation between all L_1 and dCu concentrations (Fig. 4) along with similar log K'_{Cu2+L1} values (mean 15.6 ± 0.4 across the two

Table 1
Concentrations of total dissolved copper (dCu) and copper speciation data for two stations, P4 and P26, along Line P in the NE Pacific, seafloor depths 1327 m and 4226 m respectively. L_1 and L_2 are the concentrations of the stronger and weaker copper-binding ligand classes, along with their complex stabilities (log K'_{Cu2+L} values) and the resulting free Cu^{2+} concentrations; nd = not determined. Standard deviations for dCu are from the mean of two or more measurements. Errors in L and log K'_{Cu2+L} for both classes are the standard deviation of the mean of the three fitting procedures imposed.

Station	Depth	Salinity	dCu	L_1	log	L_2	log	Cu^{2+}	pCu
	(m)		(nM)	(nM)	K'_{Cu2+L1}	(nM)	K'_{Cu2+L2}	(fM)	
P4	10	31.8	2.9 ± 0.3	3.4 ± 0.1	16.5 ± 0.1	4.3 ± 0.1	13.1 ± 0.1	0.2	15.7
	25	32.5	1.8 ± 0.3	2.0 ± 0.1	15.5 ± 0.2	7.6 ± 0.7	12.6 ± 0.6	2.2	14.7
	50	32.7	1.8 ± 0.1	2.1 ± 0.3	16.1 ± 0.4	8.7 ± 0.4	13.2 ± 0.3	0.4	15.4
	75	33.2	1.2 ± 0.1	1.2 ± 0.4	15.8 ± 0.6	20.1 ± 5.0	12.9 ± 0.4	1.1	14.9
	100	33.5	1.5 ± 0.1	1.8 ± 0.2	16.0 ± 0.2	19.7 ± 5.7	12.2 ± 0.4	0.5	15.3
	200	33.9	1.4 ± 0.1	1.6 ± 0.1	16.0 ± 0.3	5.5 ± 1.6	12.7 ± 0.9	0.5	15.3
	400	34.1	1.6 ± 0.1	1.7 ± 0.1	15.5 ± 0.2	3.8 ± 2.0	13.2 ± 0.3	2.5	14.6
	600	34.2	1.6 ± 0.1	1.8 ± 0.2	15.6 ± 0.3	1.1 ± 0.2	13.6 ± 0.3	2.0	14.7
	800	34.3	1.7 ± 0.1	2.0 ± 0.1	15.5 ± 0.1	2.9 ± 4.9	13.2 ± 0.6	1.7	14.8
	1000	34.4	2.4 ± 0.1	2.6 ± 0.2	15.8 ± 0.3	5.5 ± 0.5	13.1 ± 0.6	1.3	14.9
	1200	34.5	3.0 ± 0.2	2.8 ± 0.3	15.4 ± 0.3	7.9 ± 0.1	13.5 ± 0.4	2.6	14.6
P26	10	32.5	2.4 ± 0.1	2.7 ± 0.1	15.0 ± 0.1	3.4 ± 0.4	11.6 ± 0.5	8.8	14.1
	25	32.5	2.3 ± 0.1	2.7 ± 0.2	15.5 ± 0.2	5.0 ± 0.1	12.9 ± 0.9	1.7	14.8
	50	32.7	2.1 ± 0.1	2.3 ± 0.2	15.4 ± 0.1	4.3 ± 0.6	13.3 ± 0.4	2.0	14.7
	75	32.8	2.3 ± 0.1	2.5 ± 0.6	15.3 ± 0.2	5.2 ± 1.0	13.0 ± 0.7	3.2	14.5
	100	32.8	2.4 ± 0.1	2.5 ± 0.8	15.7 ± 0.6	7.7 ± 0.6	13.5 ± 0.2	1.2	14.9
	200	33.8	3.0 ± 0.1	3.6 ± 0.5	15.5 ± 0.3	8.0 ± 1.9	13.2 ± 0.4	1.2	14.9
	400	34	3.0 ± 0.1	3.5 ± 0.5	15.6 ± 0.4	7.2 ± 0.3	13.2 ± 0.5	1.3	14.9
	600	34.2	3.0 ± 0.3	nd	nd	nd	nd	nd	nd
	800	34.3	2.9 ± 0.2	3.7 ± 0.2	15.4 ± 0.1	6.1 ± 0.8	13.1 ± 0.7	1.4	14.9
	1000	34.4	3.1 ± 0.1	3.8 ± 0.2	15.2 ± 0.1	7.6 ± 1.5	13.2 ± 0.5	2.0	14.7
	1200	34.4	3.2 ± 0.4	3.1 ± 0.2	15.1 ± 0.1	5.3 ± 0.4	13.2 ± 0.7	5.3	14.3
	1400	34.5	3.3 ± 0.2	4.0 ± 0.2	15.1 ± 0.4			4.0	14.4

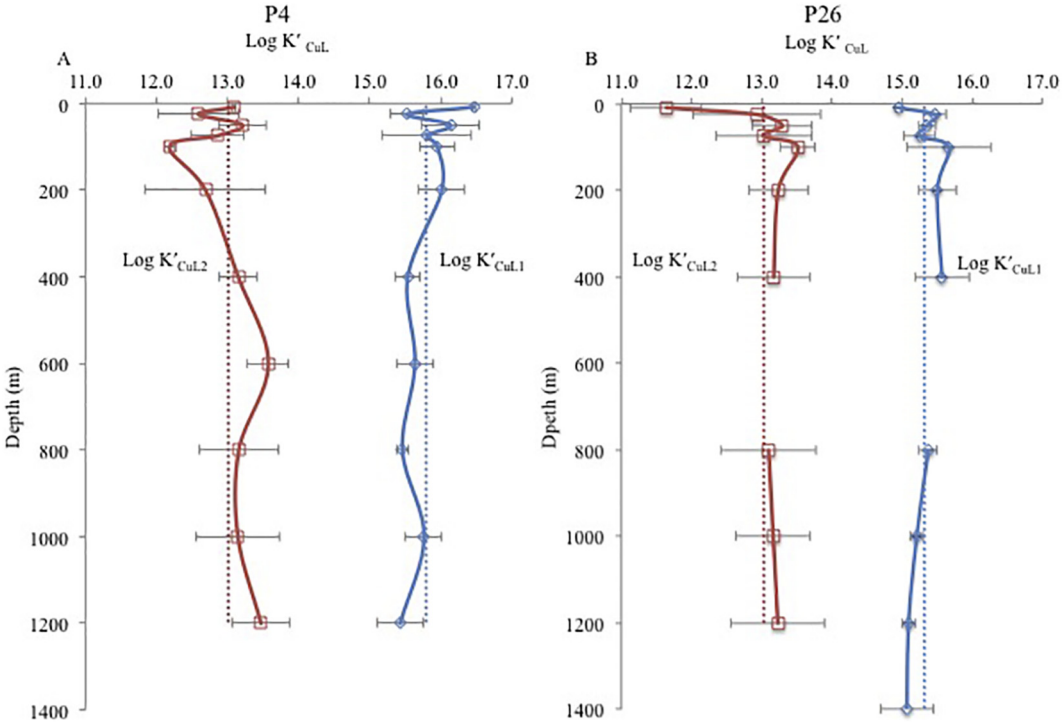

Fig. 3. Variation in log K'_{Cu2+L1} and log K'_{Cu2+L2} with depth at stations (a) P4 and (b) P26 in the NE Pacific. Dotted lines show the mean.

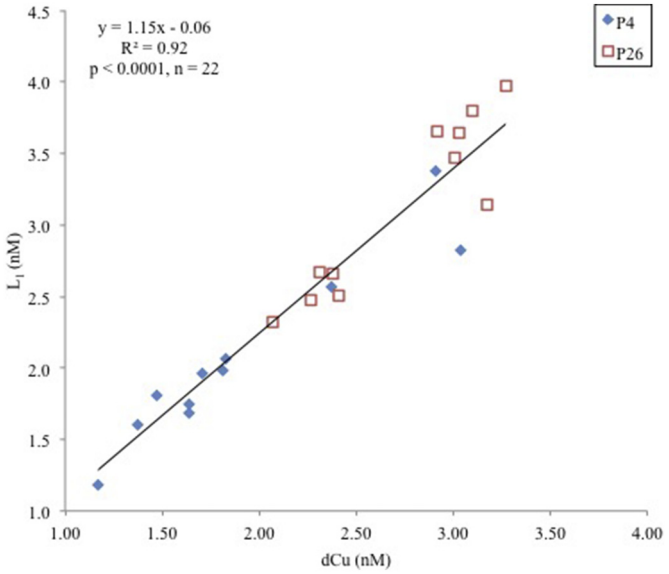

Fig. 4. The co-variation between the concentrations of dCu and L_1 for P4 and P26 in the NE Pacific. The figure shows the correlation for both stations combined. The slopes for P4 and P26 individually are y = 0.98× ± 0.2, R^2 = 0.92 and y = 1.31×-0.44, R^2 = 0.86 respectively.

stations), suggests that despite hydrographical differences, L_1 could be composed of similar compounds at both stations.

Concentrations of L_2 exceeded dCu and L_1 at all depths at both stations (except at 600 m at P4). Indeed, at P4 L_2 concentrations were quite elevated at 75 and 100 m, reaching ~20 nM, a concentration 20 times higher than the minimum measured at 600 m (Fig. 2A). These very high L_2 concentrations at P4 may be linked to inputs from the shelf (at around 200 m) or the breakdown of sinking phytoplankton. At P26, the L_2 concentration was lowest at 10 m (3.4 nM) and increased to 7.7 nM by 100 m, remaining between 6 and 8 nM down to 1000 m (Fig. 2B). The L_2 ligand class (log K'_{CuL2} 11.6–13.6) had a mean complex stability of log K'_{Cu2+L2} = 13.0 ± 0.4 at both stations (Table 1), at the high end of the typical strength of L_2 ligands (Buck and Bruland, 2005).

Previous CSV-CLE measurements have also found two ligand classes with similar log K'_{Cu2+L} values in coastal waters at higher (20 µM SA; Whitby and van den Berg, 2015) and lower detection windows (2.5 µM SA; Muller and Batchelli, 2013), as well as in surface waters of the Antarctic Peninsula at the same detection window we chose for this study (Bundy et al., 2013). The log K'_{Cu2+L} we measured for the two ligand classes (ranging 16.5–11.6) encompass those measured for a single ligand class in the euphotic zone (top 50 m) along Line P (log K'_{Cu2+L} 13.7–14.5; using a detection window centred on 5 µM SA and single ligand data fitting; Semeniuk et al., 2016b) and in surface waters of the eastern Pacific (log K'_{Cu2+L} 12.55–13.95; Boiteau et al., 2016). Studies in the NW Pacific (using 2 µM SA, a log α_{CuSA} = 4.0, and single ligand data fitting) also found log K'_{Cu2+L} values ranging between the two ligand classes found here (12.7–14.1; Moffett and Dupont, 2007), with depth profiles of L concentrations similar to our L_1 profile.

The co-variation between dCu and L_1 was tested with plots of L_1 versus dCu (Fig. 4), and was highly significant ($[L]_{nM} = [dCu]_{nM} * 1.15–0.06$, $r^2 = 0.92$, $p < 0.0001$, $n = 22$). Data from both stations follow the same line, indicating that the relationship between L_1 and dCu may be consistent from the continental slope to the open ocean in the NE Pacific.

3.4. Effect of organic complexation on the concentration of free copper (Cu^{2+})

The speciation of Cu was calculated taking both ligands into account using eq. 1 (Supplementary Information), with α_{Cu} dependent on salinity. Cu speciation was dominated by L_1, which bound, on average, 94 ± 5% of dCu. The weaker ligand class, L_2, was also important at specific depths, binding between 12 and 18% of dCu at 75 m (P4) and 100 m (P26), and at 1200 m at both stations. Due to the high complex stabilities of these two ligand classes, the calculated Cu^{2+} concentrations were very low, with an average of 1.4 ± 0.9 fM at P4 and 2.9 ± 2.3 fM at P26 (pCu 15.0 and 14.6, respectively), consistent with previous data along Line P (pCu 14.4–15.1; Semeniuk et al., 2016a) and

Table 2
Concentrations of copper-binding humic substances (HS_{Cu}) and two types of thiols (TU and GSH equivalent) for two stations, P4 and P26, along Line P in the NE Pacific (seafloor depths 1320 m and 4225 m, respectively). Each parameter as a percentage of the total ligand concentration is shown as $\%L_T$. HS_{Cu} concentrations were measured in $\mu g\,L^{-1}$ and converted to picomolar by multiplication with binding capacity of 18 pmol Cu μg^{-1} HS_{Cu} (Whitby and van den Berg, 2015). Errors show the standard deviation for the standard addition calibration, or 10% error when the value was obtained from the peak height and calibrated sensitivity. Concentrations that were below the calculated limit of detection (3× standard deviation, around 15 pM) show < LOD. HS_{Cu} values in pM are ± 10%.

Stn	Depth	HS_{Cu}	HS_{Cu}	HS_{Cu}	TU eq.	TU eq.	GSH eq.	GSH eq.
	(m)	($\mu g\,L^{-1}$)	(pM)	$\%L_T$	(pM)	$\%L_T$	(pM)	$\%L_T$
P4	10	92 ± 7	1700	21.5	140 ± 60	1.8	290 ± 29	3.8
	25	16 ± 2	290	3.0	58 ± 8	0.6	170 ± 17	1.8
	50	16 ± 2	290	2.7	32 ± 3	0.3	69 ± 7	0.6
	75	16 ± 1	290	1.3	22 ± 8	0.1	60 ± 6	0.3
	100	20 ± 1	360	1.7	60 ± 6	0.3	190 ± 10	0.9
	200	15 ± 1	270	3.9	48 ± 5	0.7	150 ± 15	2.1
	400	37 ± 3	670	12.2	< LOD		87 ± 9	1.6
	600	37 ± 3	670	23.6	29 ± 3	1.0	50 ± 5	1.8
	800	32 ± 3	580	12.0	< LOD		50 ± 5	1.0
	1000	31 ± 2	560	6.8	< LOD		31 ± 3	0.4
	1200	33 ± 2	590	5.5	< LOD		38 ± 4	0.4
P26	10	34 ± 5	610	10.0	350 ± 14	5.7	970 ± 97	15.9
	25	30 ± 5	540	7.0	295 ± 16	3.9	860 ± 86	11.2
	50	47 ± 3	850	12.8	225 ± 15	3.4	490 ± 15	7.4
	75	21 ± 5	380	4.9	270 ± 90	3.5	230 ± 23	3.0
	100	19 ± 5	340	3.3	310 ± 40	3.1	250 ± 25	2.5
	200	31 ± 5	560	4.8	452 ± 23	3.9	940 ± 94	8.0
	400	54 ± 5	970	9.1	480 ± 40	4.5	1290 ± 129	12.1
	600	35 ± 5	630		250 ± 10		610 ± 61	
	800	51 ± 3	920	9.3	211 ± 7	2.2	610 ± 61	6.2
	1000	48 ± 1	860	7.5	101 ± 10	0.9	540 ± 54	4.7
	1200	18 ± 2	320	3.8	158 ± 11	1.9	300 ± 30	3.5
	1400	33 ± 2	590	14.8	110 ± 10	2.8	580 ± 58	14.6

with findings from the North Atlantic (Jacquot and Moffett, 2015).

At P4, Cu^{2+} concentrations ranged from 0.2 to 2.6 fM (pCu 14.6–15.7), and were generally lower in the top 200 m (0.2–1 fM) than deeper than 400 m (1.3–2.6 fM). The exception was the 25 m sample with 2.2 fM [Cu^{2+}]. In contrast, at P26, the concentrations of Cu^{2+} were higher in the upper 75 m (average of 3.9 fM) than between 100 and 1000 m (average 1.4 fM Cu^{2+}). The Cu^{2+} concentrations we measured in the top 100 m (range 0.2–8.8 fM, Table 1) are comparable to those previously found at 10 m along Line P (1.7 fM at P4, 2.4 fM at P16 and 0.77 fM at P26), which were low enough to impair the photosynthetic efficiency of large phytoplankton at P26 (> 5 μm; Semeniuk et al., 2016b), but high enough to inhibit cyanobacteria and picoeukaryote growth at P16 (Semeniuk, 2014).

3.5. Copper-binding humic substances

Here we present the first depth profiles of Cu-binding humics (HS_{Cu}) in the open ocean. The HS_{Cu} concentrations ranged from 15 to 92 $\mu g\,L^{-1}$ (Table 2). Other than at 10 m, HS_{Cu} values at P4 were generally lower (mean 25 ± 9 $\mu g\,L^{-1}$ or 0.5 nM Cu binding capacity) than at P26 (mean 35 ± 12 $\mu g\,L^{-1}$ or 0.6 nM), which suggests a source of marine HS_{Cu} at P26. Marine humic-like CDOM likely originates from decaying phytoplankton (Lorenzo et al., 2007), has been found in waters from the equator to the subarctic Pacific (Yamashita and Tanoue, 2009), and binds Fe in North Pacific deep waters (Kitayama et al., 2009). Furthermore, the transport of distinct marine-derived humic substances in the mesopelagic layer is linked to the formation of NPIW in the subarctic Northwest Pacific (Yamashita and Tanoue, 2009).

In the upper 200 m, HS_{Cu} values were much more variable at P4 than P26 (15–92 vs. 19–47 $\mu g\,L^{-1}$, respectively; Fig. 5A and B). We suspect that variability in the upper waters at P4 is due to a combination of factors, including fluvial influence, high primary productivity, scavenging and photobleaching. In comparison, we find a relatively constant concentration from 400 to 1200 m at P4 (31–37 $\mu g\,L^{-1}$, around 0.6 nM Cu binding capacity), with no indication of a bottom source of HS_{Cu}, despite signs of a bottom source for dCu.

In contrast, deeper than 200 m, the concentrations of HS_{Cu} were more variable at P26 than P4 (18–54 vs. 31–37 $\mu g\,L^{-1}$, respectively; Fig. 5B, Table 2). The HS_{Cu} profile at P26 shows a similar shape to the GSH profile (Fig. 5B), possibly indicating a source from marine cell exudates (Lorenzo et al., 2007). The range of HS_{Cu} values at P26 (18–54 $\mu g\,L^{-1}$) are within the range found across the North Atlantic (10–116 $\mu g\,L^{-1}$; Whitby, unpublished) and encompass concentrations of Fe-binding humic substances (HS_{Fe}) found elsewhere in the North Pacific, (36 $\mu g\,L^{-1}$ at 1000 m; Laglera and van den Berg, 2009). For terrestrial humic substances, the concentration measured by the Fe-binding species is identical to that of the Cu-binding species, because Fe and Cu bind to the same sites on HS with similar log K values, competing for HS complexation (Abualhaija et al., 2015) and this may also hold true for the marine-derived HS detected here. The binding capacity for Fe can therefore be calculated from our HS_{Cu} values using 32 pmol Fe $\mu g\,L^{-1}$ (Laglera and van den Berg, 2009), giving around 0.5–3 nM Fe binding capacity for these HS. Humics are one of three main ligand types for Fe (Hassler et al., 2017), potentially maintaining a significant fraction of the dissolved pool of this poorly soluble element. Thus in these low Fe waters, it is possible that higher concentrations of Cu out-compete Fe for potentially important HS complexation, unless other, stronger ligands dominate Cu complexation. It is therefore essential to understand the contribution of HS in Cu complexation, particularly in HNLC regions.

3.6. Thiourea and glutathione type thiols

Across both stations, the concentrations of TU- and GSH-type thiols ranged from 22 to 480 pM and 31 to 1290 pM, respectively (Fig. 5a and b, Table 2). These values are comparable to those measured by high performance liquid chromatography (HPLC, with electrospray ionization, ESI-MS) in the subarctic Pacific Ocean (Dupont et al., 2006), where GSH reached 800 pM and another Cu-type thiol, cysteine (Cys), ranged from 300 to 2000 pM. The concentrations of GSH-type thiols in our study are also within the range of those in the North Atlantic using HPLC (< 100 to 2200 pM; Swarr et al., 2016), and are at the lower end

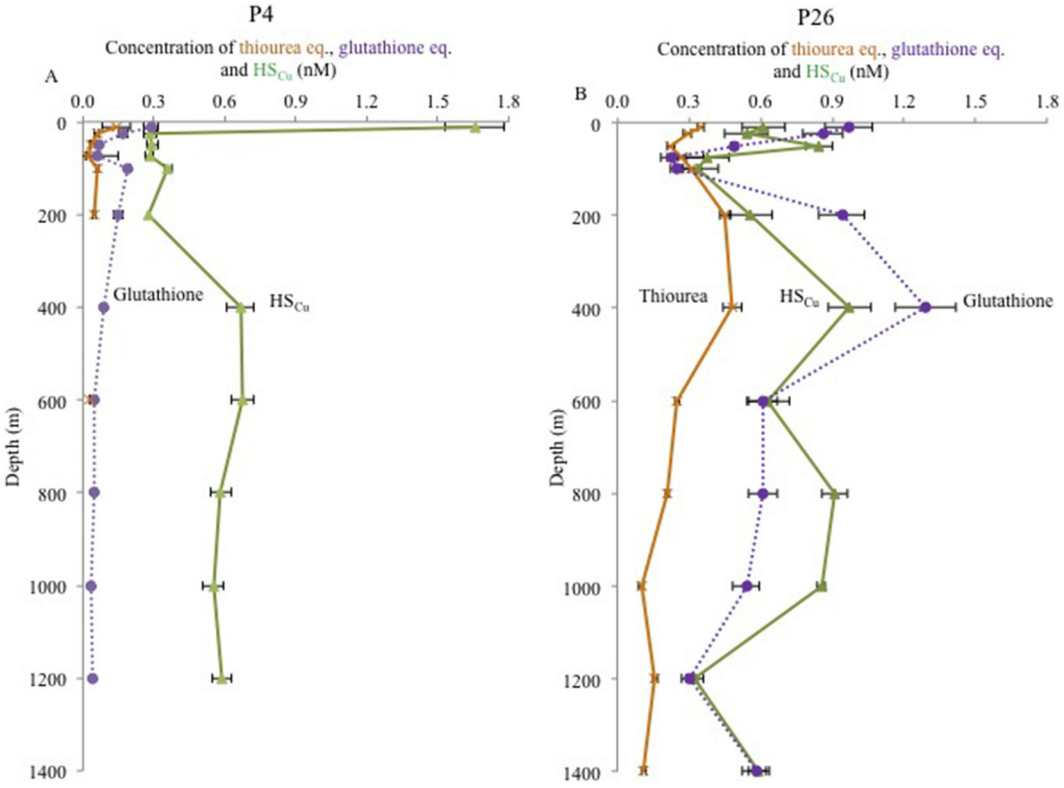

Fig. 5. Profiles of the concentrations of HS_{Cu} (green triangles) converted to nM using binding capacity of 18.0 nmol Cu mg^{-1} HS_{Cu} (Whitby and van den Berg, 2015) and thiols as TU-equivalent (orange crosses) and GSH-equivalent (purple circles), for (a) station P4 and (b) station P26 in the NE Pacific. Error bars show the standard deviation for the standard addition calibration, or 10% error when the value was obtained from the peak height and calibrated sensitivity. (For interpretation of the references to colour in this figure legend, the reader is referred to the web version of this article.)

of previous CSV measurements in the North Atlantic (< 200 pM to 15 nM; Le Gall and van den Berg, 1998).

Within the euphotic zone (top 110 m) the TU-equivalent profiles were a similar shape for both P4 and P26. However, the concentration of TU-type thiols was lower at P4, sometimes below the limit of detection, especially when the voltammetric thiol peak resembled GSH (Fig. 5A, Table 2). Concentrations of GSH-type thiols were also lower at P4 (31–290 pM) than at P26 (230–1290 pM, Fig. 5A and B), in line with higher concentrations of other RSS such as dimethylsulfide (DMS) and dimethylsulfoniopropionate (DMSP) at P26 (Asher et al., 2017), linked to oxidative stress experienced by Fe limited phytoplankton. Given that phytoplankton enhance the release of thiols and phytochelatins (GSH-containing compounds) under high dCu (Dupont and Ahner, 2005), the higher concentrations of thiols in surface waters at P26 than P4 might indicate that some phytoplankton at P26 are experiencing high Cu stress, as suggested for cyanobacteria and picoeukaryotes at P16 (Semeniuk, 2014). Compounds electrochemically similar to GSH and TU have been found to be released by *Emiliania huxleyi* in response to increasing dCu concentrations (Leal et al., 1999).

Recent studies demonstrate that the presence of certain thiols, such as GSH and Cys, may actually increase the bioavailability of dCu (Walsh et al., 2015). This is because the high-affinity Cu transport system in some eukaryotic phytoplankton is dependent on Cu^{+} (Guo et al., 2015; Semeniuk et al., 2009) and thiols, such as Cys, have been shown to increase its concentration at the cell surface by a thiol-mediated reductive dissociation of strong Cu^{2+} organic complexes (Walsh et al., 2015). Furthermore, in a previous study at P26, the addition of a variety of weak Cu(I) ligands, including thiols, enhanced dCu uptake, which could be explained by cell surface enzymes reducing Cu(II) to Cu (I), or by ligand exchange between weak Cu-binding ligands and the cellular Cu transporters (Semeniuk et al., 2015). Thiols may thus be able to, depending on phytoplankton taxa, enhance uptake or reduce toxicity of Cu^{2+}. A previous study at P26 suggests that low Cu^{2+} concentrations limit the photosynthetic activity in larger phytoplankton (Semeniuk et al., 2016b). Thus, we suggest that the thiols at P26 might be released by high Cu stressed cyanobacteria, but may enhance uptake of Cu(I) by larger phytoplankton.

3.7. Composition of the L_2 ligand class

Log K'_{Cu2+L} values of thiols range from 10 to 14, with GSH around 12 to 13 (Leal and van den Berg, 1998; Walsh and Ahner, 2013). Natural organic ligands suspected to be thiols have also been found with log K'_{Cu2+L} values of 12.3–15 (Laglera and van den Berg, 2003; Sander et al., 2007; Whitby et al., 2017). Different thiols could therefore potentially contribute to the L_2 ligand class in our samples where log K'_{Cu2+L2} ranges from 11.6 to 13.6. The concentration of L_2 was generally highest around 100 m, especially at P4, suggesting a biological source, similar to subsurface thiol production in the North Atlantic (Swarr et al., 2016). In addition, if the ligands in the L_2 class were thiols, their photo-oxidation might explain the lower L_2 concentrations we measured at the shallowest depths, given that some thiols are photoreactive (Laglera and van den Berg, 2006). However, the concentrations of TU and GSH did not co-vary with those of L_2 (Supplementary Fig. 2), and were significantly lower (only 0.5–28% of L_2). This latter result suggests that other compounds (potentially other thiols and/or phytochelatins) make up the largest portion of the L_2 ligand class.

HS_{Cu} have a log K'_{Cu2+L} around 12 (Whitby and van den Berg, 2015) and have been found to correlate very well with L_2 in estuaries (Whitby et al., 2017). However, similar to the thiols, here we do not see significant correlations between HS_{Cu} concentrations and L_2 at either station (Supplementary Fig. 3B and D), with HS_{Cu} ranging from 1.4–61% of L_2 (data not shown). In summary, even though HS_{Cu} and some GSH-like thiols are likely contributing to the L_2 ligand class, some

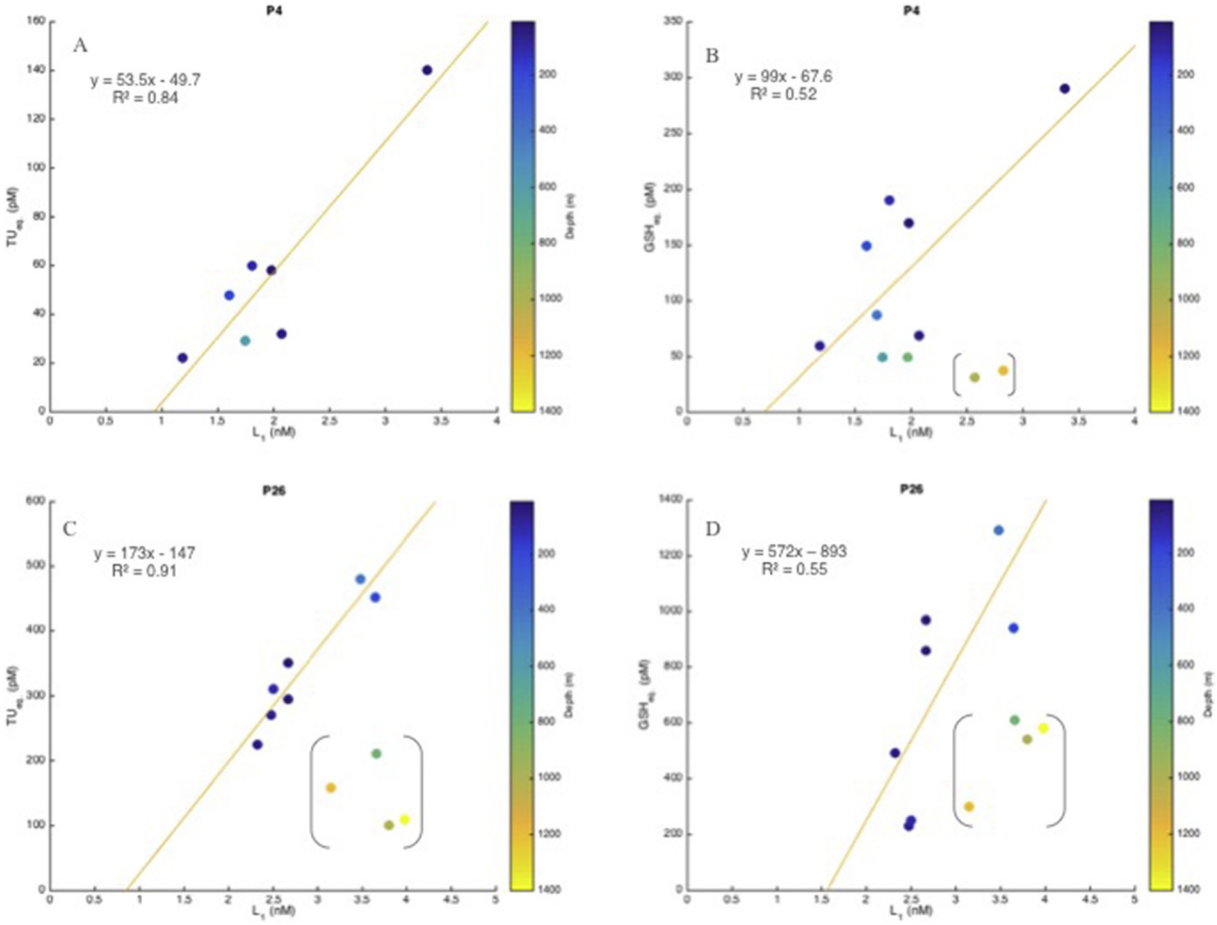

Fig. 6. The relationship between the concentrations of thiols and L_1, colour coded to show variation with depth. Top panels (a and b) are P4, bottom panels (c and d) are P26. (a) TU-type and L_1 at P4, (b) GSH-type and L_1 at P4; (c) TU-type and L_1 at P26; (d) GSH-type and L_1 at P26. Slopes do not include some values from the OMZ, shown in brackets.

important Cu-binding ligands (with log K'_{Cu2+L2} between 11.6 and 13.6) remain to be determined.

3.8. Composition of the L_1 ligand class

We found that most of the dCu (around 94%) was bound to L_1, with significant correlation between the concentrations of dCu and L_1 (Fig. 4). Furthermore, when some of the OMZ samples were omitted, the concentrations of TU were well correlated with those of L_1 (Fig. 6). This is similar to recent findings for surface samples from an estuary (Whitby et al., 2017). However, the low concentrations of TU-type thiols found here mean that these thiols would only contribute between 1 and 14% to the L_1 pool, which if combined with GSH-type (more likely to be L_2) could account for 1 to 50% of L_1.

Low concentrations of very strong ligands could contribute to the L_1 ligand class without being distinguished as a separate ligand, since ligand concentrations and stability constants are in fact weighted averages of all ligands within that detection window (Miller and Bruland, 1997). For example, even a very low concentration of chalkophores (the strongest Cu-ligands known in nature) could influence log K'_{Cu2+L1} values. Chalkophores are high affinity, Cu-complexing agents analogous to siderophores for Fe, such as methanobactins, secreted by specific methane-oxidizing bacteria when grown under low Cu (DiSpirito et al., 2016; Hakemian et al., 2005). Preliminary evidence has been gathered in support of marine heterotrophic bacteria as a source of organic Cu ligands along Line P (Semeniuk et al., 2016b), but the effect of chalkophores on metal speciation and bioavailability in natural systems has yet to be established. Methanotrophs occupy a plethora of habitats, including estuaries, open ocean waters (Sieburth et al., 1987; Smith et al., 1997) and hydrothermal vents (Duperron et al., 2006). A recent review suggests methanobactin biosythesis may be much more widespread than originally thought, potentially beyond methane oxidizers (Dassama et al., 2017). Methanobactins are multidentate ligands that contain sulphur carbonyl (thiourea- and thioamide-based) functional groups bound to a hydroimidazole group with log K'_{Cu2+L} values around 18.8 (Choi et al., 2006; El Ghazouani et al., 2012), although to our knowledge the CSV response of these compounds has not been tested.

3.9. Contribution of thiols and HS_{Cu} to the total ligand pool

To investigate the possible contribution of TU, GSH and HS_{Cu} to dCu complexation, we plotted their concentrations relative to that of the total ligand (L_T), as a % of L_T, against depth (Supplementary Fig. 4A and B). At P4, the contribution of HS_{Cu} dominates and is highest at the surface and at the top of the OMZ (at 600 m), implying inputs from riverine sources and processes within the OMZ (Supplementary Fig. 4A). In contrast, at P26, GSH and HS_{Cu} contribute similarly to L_T. The sum of their contributions (TU, GSH and HS_{Cu}) is slightly higher at P26 (9–32%) than at P4 (2–27%), but both stations exhibit similar depth profile trends (Supplementary Fig. 5). Thus, the factors controlling the ligands contributing to dCu complexation may be relatively consistent across different regions, despite variation in sources and sinks of both dCu and ligands between the continental slope station and the HNLC station in the NE Pacific.

In oligotrophic waters of the eastern Pacific, 6–20% of the dCu was

complexed by humic-like compounds and a thiol-containing compound (Boiteau et al., 2016). Here, we similarly find HS_{Cu} and thiol-like ligands contributing to 2–32% of the total ligand pool (Table 2, Supplementary Fig. 5). Boiteau et al. (2016) identified a multidentate ligand—with the molecular formula of $[C_{20}H_{21}N_4O_8S_2 + M]^+$ including a thiol-like sulphur group—that accounted for 4 to 5% of dCu in open ocean surface samples. Similarly here, we find that the TU-like thiols contribute 4 to 6% of L_T in surface ocean waters (10–25 m at P26, Table 2, Supplementary Fig. 4). We speculate that the TU-type thiol peak we see in the voltammetric scans could be a thiocarbonyl (sulphur carbonyl) within a larger compound (such as a methanobactin or porphyrin) rather than free thiourea, for which there are no known marine sources. This could explain why TU correlates best with the L_1 ligand class with a stronger binding strength than typical thiols, since Cu complexation could be through N atoms of cyclic azole-like functional groups at the other end of the molecule (Boiteau et al., 2016). These combined results imply that very strong Cu-binding compounds, such as chalkophores, may contribute to organic complexation of dCu in the ocean.

Although electrochemical measurements do not provide direct information on ligand structures, the agreement on the percentage of humic-like and thiol-like compounds complexing dCu in surface waters between these independent methods is promising. Further work is needed to test the electrochemical response of methanobactins, peptides, porphyrins and isolated natural ligands against voltammetric peaks observed in natural seawater.

3.10. Attempting to identify the other thiol peaks

In most samples, a single thiol peak was present at around E = −0.53 V, which responded to additions of GSH and TU and was used to measure the thiol concentration in GSH and TU equivalents. Thioacetamide gives a similar peak to TU (also Hg-type) and thus could also have been used for the TU-type thiol measurements, as the same concentrations are obtained at E_{dep} = +0.05 V (Whitby et al., 2017). Cysteine and methanethiol were tested but neither increased the peak at −0.53 V, both producing new peaks at more positive potentials of E = −0.34 and −0.37 V, respectively. Previous work has shown that allylthiourea, 2-mercaptoethanol, and 3-mercaptopropionic acid also give peaks at more positive potentials, and dimethyl sulphide does not show a peak at these conditions (Casassas et al., 1985; Laglera and van den Berg, 2003; Whitby et al., 2017). However, in some samples, other peaks were visible after manipulation of the deposition potential and other parameters. A series of tests were performed in an attempt to characterise these other peaks, on a 75 m sample from P26 (Supplementary Table 1). After a long deposition time (300 s) and depending on the deposition potential, up to three separate peaks could be distinguished, suspected to be thiols, sometimes occurring simultaneously or coalescing (Supplementary Fig. 1A).

The peak position of the three separate suspected thiols are shown in Supplementary Table 1, along with the optimum deposition potential for each suspected thiol peak and the response to additions of TU, GSH and Cu. In summary: peak 1, at E = −0.30 V (similar to either cysteine or 3-mercaptopropionic acid) was only visible after background subtraction or a long (300 s) deposition time. Tests with additions of 3 nM cysteine doubled the peak height. However, cysteine is a Cu-thiol type peak and addition of Cu to the sample did not increase this peak, as would be expected for Cu-Cys (Leal and van den Berg, 1998). Therefore, peak 1 could also be combination of similar thiols, such as cysteine and 3-mercaptopropionic acid. Although the HS peak is in a similar region at −0.24 V, HS do not show a peak until copper is added (30 nM, Supplementary Fig. 1B) and have an optimum deposition potential of +0.05 V. Peak 2, at E = −0.43 V, also only became visible after background subtraction or a long (300 s) deposition time. This peak had an optimum E_{dep} of +0.05 V and did not respond to Cu additions, suggesting a Hg-species, consistent with a TU-type thiol. However, Peak 2 decreased in response to TU additions, suggesting that TU competed with the unknown species for Hg. Peak 2 could potentially be 2-mercaptoethanol, which has a peak position of around E = −0.4 V (Casassas et al., 1985). Peak 3 at E = −0.53 V was the largest peak and the only peak consistently present with or without background subtraction and at shorter deposition times, suggesting a higher concentration, and was the peak used for all thiol measurements presented in GSH and TU equivalents. Peak 3 had an optimum E_{dep} of −0.2 V (suggestive of an adsorptive Cu-species) and increased in response to Cu and GSH additions, suggesting it is composed of GSH, but also responded to additions of TU. In some samples (e.g. P26, 800 m), this peak appeared to be a "double peak" before addition of either standard, with both the broad GSH peak and a sharp TU-type shoulder penetrating the top of the peak, suggesting coalescing of both GSH-type and TU-type thiols.

3.11. Caveats, assumptions and other considerations

Voltammetry cannot definitively distinguish between similar thiol types. Although Peak 3 responded to additions of both TU and GSH, the thiol in the samples did not behave identically to either standard suggesting it was composed of a combination of GSH-like and TU-like thiols coalescing. It is possible that during CSV, some glutathione-rich phytochelatins dissociate and release GSH at the electrode surface during the deposition step. Other similar thiols and phytochelatins contributing to the measured peak could influence the initial peak height and influence the concentrations obtained, and so we do not propose that we are measuring TU or GSH directly but rather the concentrations of Hg and Cu-binding types in TU and GSH equivalents, respectively. Furthermore, up to three separate potential thiol peaks could be distinguished after background subtraction in the sample tested (P26, 75 m). Additional potential thiols that bind Cu that may have been present include ovothiol, ergothioneine, mercaptoacetic acid and mercaptosuccinic acid, as well as various phytochelatins and folic acid (Ahner et al., 1998; De Luna et al., 2013; Dryden et al., 2007). Whilst we cannot conclusively determine the identity of the thiols in our samples, GSH and TU are likely good model ligands for Peak 3 (E = −0.53 V) given that they represent the two main thiol peak types (Cu-thiol and Hg-thiol) at that potential when measuring with CSV. Future electrochemical measurements on thiols should involve repeatedly shifting the deposition potential and Cu saturation to better distinguish between coalescing thiols (Laglera and Tovar-Sanchez, 2012) and be used in conjunction with other methods such as HPLC (Tang et al., 2000).

The fact that glutathione can undergo oxidation in the presence of Cu(II) (Moingt et al., 2010), raises a question about whether our GSH-type thiol values could be underestimated. However, we anticipate that ready-complexed GSH would be relatively resistant to oxidation, and indeed the GSH-like thiol peak in the voltammogram scans remained stable across numerous repeat scans (except for some samples within the OMZ), thus supporting no loss of GSH during our measurements. TU measurements do not have this problem as they are obtained without addition of Cu. Thiols form complexes with Cu at different metal to ligand ratios (e.g. 1:1, 2:1) depending on the thiol type and on conditions, such as pH, making it difficult to conclusively compare thiol concentrations to the ligand classes directly. Furthermore, obtaining ligand data from CLE-CSV titrations has limitations. The ligand concentrations are based on the detection window selected, and as discussed, the log K'_{Cu2+L} values represent an average of the ligand classes within the detection window. Samples were filtered and thus do not include reactions with particulate Cu. Although we equilibrated for a minimum of 8 h, which should be sufficient for most complexes, without additional kinetic data for slower kinetic interactions it is difficult to fully interpret ligand trends.

No systematic difference was observed in the voltammetric response for humic substances from different samples, suggesting that the HS_{Cu}

group in the molecules that is detected is common in all. Nevertheless, it is feasible that marine-derived humic material from different sources may have a different overall composition that is not detected by voltammetry. This could lead to under- or overestimation of the conversion to concentration in nM using values based on a terrestrial humic standard, and marine HS could potentially have a different log K'_{Cu2+L}. Despite probable differences between the structures and characteristics of marine and terrestrial humic substances, the binding capacity of Cu for HS_{Cu} from riverine and offshore sediments has been found to remain constant (log K'_{Cu2+L} 11.4–11.9; (Sohn and Weese, 1986), and similar to estuarine waters (log K'_{Cu2+L} 12; Whitby and van den Berg, 2015), suggesting that the complexing capacity of marine-derived humic substances in seawater may also be comparable to that of terrestrial standards. Future studies should involve isolating humic material for testing the binding capacity in a wider range of sample types. Separating humic substances into terrestrial and marine-derived fractions can be achieved using excitation emission matrix fluorescence and parallel factor analysis (EEM-PARAFAC) (Yamashita and Jaffe, 2008) and combining this technique with voltammetry may be useful for the characterization of humic substances in future studies.

Finally, a reduction peak at −0.1 V was found to interfere with the measurement of HS_{Cu} in surface samples (10, 25 and 50 m) at P26, which was ascribed to iodide as the peak increased with the addition of iodide. This peak was not present in samples from other depths at P26 and not in any of the samples from P4. Iodide, a biophilic trace element (Wong, 1991) is produced by photochemical and microbial reduction of iodate (Wong et al., 2002), potentially mediated by bacterial nitrate reductase (Tsunogai and Sase, 1969). Although the purpose of iodate reduction remains unclear, observations support a linkage with nitrate uptake (Campos et al., 1999). Although this peak interfered with the HS_{Cu} peak height measurement, the effect was consistent and the standard additions were linear, therefore we do not think it influenced the results at these three depths.

4. Conclusions

Our work suggests that Cu is strongly complexed by two ligands throughout the water column at both P4 and P26 in this HNLC region. Dissolved Cu concentrations are primarily controlled (81.4–99.6%) by a single strong ligand class (L_1) of log K'_{Cu2+L1} 15–16.5, which co-varied with dCu at all depths. The remaining dCu was bound by a weaker ligand class (log K'_{Cu2+L2} 11.6–13.6), which was generally found at much higher concentrations than L_1. The combination of both ligand classes resulted in very low concentrations of Cu^{2+} (0.2–8.8 fM, pCu 14.1–15.7) throughout the water column at both stations.

GSH-like and TU-like thiols, along with HS_{Cu}, were found to represent a proportion of the ligands. The complex stability of L_2 is similar to that of GSH-type thiols and terrestrial HS_{Cu}. TU-type thiol concentrations correlated better with L_1 than with L_2. Overall, HS_{Cu} are suspected to be marine derived, and contributed to 1–27% (on average 9%) of L_T, and when combined with the two thiols contributed to up to 32% of L_T (on average 15%). Since the concentrations of both L_1 and L_2 were greater than those of the humic substances and thiols combined, other ligand types are likely responsible for the majority of dCu complexation in these waters. Some potential candidates for the detected, but unidentified, thiols are cysteine, 3-mercaptopropionic acid and 2-mercaptoethanol, all of which bind Cu. In support of our hypothesis, cysteine, and 3-mercaptopropionic acid have been detected previously in natural waters (Dupont et al., 2006; Hu et al., 2006).

A marked variation between TU-like thiols, GSH and HS_{Cu} concentrations at the surface, mid-depths, and deep waters suggests these compounds are likely to be contributing to the ligand pools but in small and inconsistent fractions, likely influenced by surface processes, the OMZ and other factors. The presence of thiocarbonyls in known chalkophores and in strong Cu-ligands characterized in other parts of the eastern Pacific, along with our correlation between TU-like thiol and L_1, tentatively suggest that the electrochemical TU-type peak could be part of a larger, unidentified Cu-binding compound with a stronger binding strength than typical thiols, such as a methanobactin or porphyrin. This, along with the high log K'_{Cu2+L1} values, could suggest that chalkophores play a greater role in oceanic dCu complexation than previously considered, and future work should examine the voltammetric response of such compounds. Electrochemical methods should be combined with other techniques, such as HPLC-ESI-MS and EEM-PARAFAC, to further advance our knowledge on the structural characterization of ligands from seawater and laboratory cultures. Although the exact composition of the ligand classes remains unknown, we have provided an insight into some promising key components contributing to Cu complexation in oceanic waters.

Supplementary data to this article can be found online at https://doi.org/10.1016/j.marchem.2018.05.008.

Acknowledgements

We thank participants of the August 2012 Line P cruise, especially chief scientist Marie Robert, the trace metal sampling teams Christina Schallenberg and Dave Janssen, and the captains and crew of the CCGS J.P. Tully. We also thank David Semeniuk for his advice on Cu trends in this region, Sioned Mai Davies and two anonymous reviewers for their insightful and constructive comments. Hannah Whitby was supported by a scholarship of the Natural Environment Research Council (NE/K500975/1). Van den Berg is grateful for on-going support from the University of Liverpool, where the experimental work was carried out.

References

Abualhaija, M.M., Whitby, H., van den Berg, C.M.G., 2015. Competition between copper and iron for humic ligands in estuarine waters. Mar. Chem. 172, 46–56.
Ahner, B.A., Lee, J.G., Price, N.M., Morel, F.M.M., 1998. Phytochelatin concentrations in the equatorial Pacific. Deep-Sea Res. Part I 45 (11), 1779–1796.
Allen, H.E., Matson, W.R., Mancy, K.H., 1970. Trace metal characterization in aquatic environments by anodic stripping voltammetry. J. Water Pollution Contr. Federation 42 (4), 573–581.
Amin, S.A., et al., 2013. Copper requirements of the ammonia-oxidizing archaeon Nitrosopumilus maritimus SCM1 and implications for nitrification in the marine environment. Limnol. Oceanogr. 58 (6), 2037–2045.
Annett, A.L., Lapi, S., Ruth, T.J., Maldonado, M.T., 2008. The effects of Cu and Fe availability on the growth and Cu: C ratios of marine diatoms. Limnol. Oceanogr. 53 (6), 2451–2461.
Asher, E., Dacey, J.W., Ianson, D., Peña, A., Tortell, P.D., 2017. Concentrations and cycling of DMS, DMSP, and DMSO in coastal and offshore waters of the Subarctic Pacific during summer, 2010-2011. J. Geophys. Res. 122 (4), 3269–3286.
Averett, R.C., Leenheer, J.A., McKnight, D.M., Thorn, K.A., 1994. Humic substances in the Suwannee River, Georgia: interactions, properties, and proposed structures. U.S. Geol. Water-Supply Paper 2373.
de Baar, H.J.W., et al., 2005. Synthesis of iron fertilization experiments: from the iron age in the age of enlightenment. J. Geophys. Res. 110 (C9).
Benner, R., 2002. Chemical composition and reactivity. In: Biogeochemistry of Marine Dissolved Organic Matter. Elsevier, San Diego, CA, USA.
Boiteau, R.M., et al., 2016. Structural characterization of natural nickel and copper binding ligands along the US GEOTRACES eastern Pacific zonal transect. Front. Mar. Sci. (243), 3.
Boyd, P.W., 2007. Biogeochemistry - iron findings. Nature 446 (7139), 989–991.
Boyle, E.A., Sclater, F.R., Edmond, J.M., 1977. The distribution of dissolved copper in the Pacific. Earth Planet. Sci. Lett. 37 (1), 38–54.
Brand, L.E., Sunda, W.G., Guillard, R.R.L., 1986. Reduction of marine-phytoplankton reproduction rates by copper and cadmium. J. Exp. Mar. Biol. Ecol. 96 (3), 225–250.
Bruland, K.W., 1980. Oceanographic distributions of cadmium, zinc, nickel, and copper in the North Pacific. Earth Planet. Sci. Lett. 47 (2), 176–198.
Bruland, K.W., Rue, E.L., Donat, J.R., Skrabal, S.A., Moffett, J.W., 2000. Intercomparison of voltammetric techniques to determine the chemical speciation of dissolved copper in a coastal seawater sample. Anal. Chim. Acta 405 (1–2), 99–113.
Bruland, K.W., Middag, R., Lohan, M.C., 2014. Controls of trace metals in seawater. In: Turekian, H.D.H.K. (Ed.), Treatise on Geochemistry, Second Edition. Elsvier, Oxford, pp. 19–51.
Buck, K.N., Bruland, K.W., 2005. Copper speciation in San Francisco Bay: a novel approach using multiple analytical windows. Mar. Chem. 96 (1–2), 185–198.
Buck, K.N., Ross, J.R.M., Flegal, A.R., Bruland, K.W., 2007. A review of total dissolved copper and its chemical speciation in San Francisco Bay, California. Environ. Res. 105 (1), 5–19.
Buck, K.N., et al., 2012. The organic complexation of iron and copper: an intercomparison of competitive ligand exchange-adsorptive cathodic stripping voltammetry (CLE-

ACSV) techniques. Limnol. Oceanogr. 10, 496–515.
Bundy, R.M., Barbeau, K.A., Buck, K.N., 2013. Sources of strong copper-binding ligands in Antarctic Peninsula surface waters. Deep-Sea Res. Part II 90, 134–146.
Bundy, R.M., et al., 2015. Iron-binding ligands and humic substances in the San Francisco Bay estuary and estuarine-influenced shelf regions of coastal California. Mar. Chem. 173, 183–194.
Campos, M., van den Berg, C.M.G., 1994. Determination of copper complexation in seawater by cathodic stripping voltammetry and ligand competition with salicylaldoxime. Anal. Chim. Acta 284 (3), 481–496.
Campos, M.L.A.M., Sanders, R., Jickells, T., 1999. The dissolved iodate and iodide distribution in the South Atlantic from the Weddell Sea to Brazil. Mar. Chem. 65 (3–4), 167–175.
Casassas, E., Arino, C., Esteban, M., 1985. Cathodic stripping voltammetry of 2-mercaptoethanol. Anal. Chim. Acta 176 (Oct), 113–119.
Choi, D.W., et al., 2006. Spectral, kinetic, and thermodynamic properties of Cu(I) and Cu (II) binding by methanobactin from methylosinus trichosporium OB3b. Biochemistry 45 (5), 1442–1453.
Coale, K.H., Bruland, K.W., 1988. Copper complexation in the Northeast Pacific. Limnol. Oceanogr. 33, 1084–1101.
Cullen, J.T., Chong, M., Ianson, D., 2009. British Columbian continental shelf as a source of dissolved iron to the subarctic northeast Pacific Ocean. Glob. Biogeochem. Cycles 23.
Cutter, G., et al., 2010. Sampling and Sample-Handling Protocols for GEOTRACES Cruises.
Dassama, L.M.K., Kenney, G.E., Rosenzweig, A.C., 2017. Methanobactins: from genome to function. Metallomics 9 (1), 7–20.
De Luna, P., Bushnell, E.A.C., Gauld, J.W., 2013. A density functional theory investigation into the binding of the antioxidants ergothioneine and ovothiol to copper. J. Phys. Chem. A 117 (19), 4057–4065.
van den Berg, C.M.G., 1982a. Determination of copper complexation with natural organic ligands in seawater by equilibration with MnO_2 II. Experimental procedures and application to surface seawater. Mar. Chem. 11 (4 SU), 323–342.
van den Berg, C.M.G., 1982b. Determination of copper complexation with natural organic-ligands in sea-water by equilibration with MnO_2. 1. Theory. Mar. Chem. 11 (4), 307–322.
van den Berg, C.M.G., 2014. UV digestion apparatus [Online]. Available: http://pcwww.liv.ac.uk/~sn35/Site/UV_digestion_apparatus.html.
DiSpirito, A., et al., 2016. Methanobactin and the link between copper and bacterial methane oxidation. Microbiol. Mol. Biol. Rev. 80 (387), 409.
Dryden, C.L., Gordon, A.S., Donat, J.R., 2007. Seasonal survey of copper-complexing ligands and thiol compounds in a heavily utilized, urban estuary: Elizabeth River, Virginia. Mar. Chem. 103 (3–4), 276–288.
Duperron, S., et al., 2006. A dual symbiosis shared by two mussel species, Bathymodiolus azoricus and Bathymodiolus puteoserpentis (Bivalvia: Mytilidae), from hydrothermal vents along the northern Mid-Atlantic Ridge. Environ. Microbiol. 8 (8), 1441–1447.
Dupont, C.L., Ahner, B.A., 2005. Effects of copper, cadmium, and zinc on the production and exudation of thiols by *Emiliania huxleyi*. Limnol. Oceanogr. 50 (2), 508–515.
Dupont, C.L., Moffett, J.W., Bidigare, R.R., Ahner, B.A., 2006. Distributions of dissolved and particulate biogenic thiols in the subartic Pacific Ocean. Deep-Sea Res. Part I 53 (12), 1961–1974.
El Ghazouani, A., et al., 2012. Variations in methanobactin structure influences copper utilization by methane-oxidizing bacteria. Proceed. Natl. Acad. Sci. U.S.A. 109 (22), 8400–8404.
Ertel, J.R., Hedges, J.I., 1983. Bulk chemical and spectroscopic properties of marine and terrestrial humic acids, melanoidins and catechol-based synthetic polymers. In: Christmas, R.F., Gjessing, E.T. (Eds.), Aquatic and Terrestrial Humic Materials. Ann Arbor Science, Ann Arbor, pp. 143–162.
Gerringa, L.J.A., Herman, P.M.J., Poortvliet, T.C.W., 1995. Comparison of the linear van den Berg Ruzic transformation and a nonlinear fit of the Langmuir isotherm applied to Cu speciation data in the estuarine environment. Mar. Chem. 48 (2), 131–142.
Guo, J., Lapi, S., Ruth, T.J., Maldonado, M.T., 2012. The effects of iron and copper availability on the copper stoichiometry of marine phytoplankton. J. Phycol. 48 (2), 312–325.
Guo, J., Green, B.R., Maldonado, M.T., 2015. Sequence analysis and gene expression of potential components of copper transport and homeostasis in *Thalassiosira pseudonana*. Protist 166 (1), 58–77.
Hakemian, A.S., et al., 2005. The copper chelator methanobactin from *Methylosinus trichosporium* OB3b binds copper(I). J. Am. Chem. Soc. 127 (49), 17142–17143.
Harvey, G.R., Boran, D.A., Chesal, L.A., Tokar, J.M., 1983. The structure of marine fulvic and humic acids. Mar. Chem. 12 (2–3), 119–132.
Hassler, C., van den Berg, C.M.G., Boyd, P.W., 2017. Toward a regional classification to provide a more inclusive examination of the ocean biogeochemistry of iron-binding ligands. Front. Mar. Sci. 4, 19–60.
Heller, M.I., Gaiero, D.M., Croot, P.L., 2013. Basin scale survey of marine humic fluorescence in the Atlantic: relationship to iron solubility and H_2O_2. Glob. Biogeochem. Cycles 27 (1), 88–100.
Hu, H., Mylon, S.E., Benoit, G., 2006. Distribution of the thiols glutathione and 3-mercaptopropionic acid in Connecticut lakes. Limnol. Oceanogr. 51 (6), 2763–2774.
Jacquot, J.E., Moffett, J.W., 2015. Copper distribution and speciation across the International GEOTRACES Section GA03. Deep-Sea Res. II Top. Stud. Oceanogr. 116, 187–207.
Jacquot, J.E., Kondo, Y., Knapp, A.N., Moffett, J.W., 2013. The speciation of copper across active gradients in nitrogen-cycle processes in the eastern tropical South Pacific. Limnol. Oceanogr. 58 (4), 1387–1394.
Janssen, D.J., Cullen, J.T., 2015. Decoupling of zinc and silicic acid in the subarctic northeast Pacific interior. Mar. Chem. 177, 124–133.
Kieber, R.J., Hydro, L.H., Seaton, P.J., 1997. Photooxidation of triglycerides and fatty acids in seawater: implication toward the formation of marine humic substances. Limnol. Oceanogr. 42 (6), 1454–1462.
Kies, L., Fast, T., Wolfstein, K., Hoberg, M., 1996. On the role of algae and their exopolymers in the formation of suspended particulate matter in the Elbe estuary (Germany). Adv. Limnol. 47 (47), 93–103.
Kitayama, S., et al., 2009. Controls on iron distributions in the deep water column of the North Pacific Ocean: Iron(III) hydroxide solubility and marine humic-type dissolved organic matter. J. Geophys. Res. 114.
Kogut, M.B., Voelker, B.M., 2001. Strong copper-binding behavior of terrestrial humic substances in seawater. Environ. Sci. Technol. 35 (6), 1149–1156.
Laglera, L.M., Tovar-Sanchez, A., 2012. Direct recognition and quantification by voltammetry of thiol/thioamide mixes in seawater. Talanta 89, 496–504.
Laglera, L.M., van den Berg, C.M.G., 2003. Copper complexation by thiol compounds in estuarine waters. Mar. Chem. 82 (1–2), 71–89.
Laglera, L.M., van den Berg, C.M.G., 2006. Photochemical oxidation of thiols and copper complexing ligands in estuarine waters. Mar. Chem. 101 (1–2), 130–140.
Laglera, L.M., van den Berg, C.M.G., 2009. Evidence for geochemical control of iron by humic substances in seawater. Limnol. Oceanogr. 54 (2), 610–619.
Lam, P.J., Bishop, J.K.B., Henning, C.C., Marcus, M.A., Waychunas, G.A., Fung, I.Y., 2006. Wintertime phytoplankton bloom in the subarctic Pacific supported by continental margin iron. Glob. Biogeochem. Cycles 20, GB1006. http://dx.doi.org/10.1029/2005GB002557.
Le Gall, A.-C., van den Berg, C.M.G., 1998. Folic acid and glutathione in the water column of the North East Atlantic. Deep-Sea Res. Part I 45, 1903–1918.
Leal, M.F.C., van den Berg, C.M.G., 1998. Evidence for strong copper(I) complexation by organic ligands in seawater. Aquat. Geochem. 4 (1), 49–75.
Leal, M.F.C., Vasconcelos, M., van den Berg, C.M.G., 1999. Copper-induced release of complexing ligands similar to thiols by *Emiliania huxleyi* in seawater cultures. Limnol. Oceanogr. 44 (7), 1750–1762.
Little, S.H., Vance, D., Siddall, M., Gasson, E., 2013. A modeling assessment of the role of reversible scavenging in controlling oceanic dissolved Cu and Zn distributions. Glob. Biogeochem. Cycles 27 (3), 780–791.
Lorenzo, J.I., Nieto-Cid, M., Alvarez-Salgado, X.A., Perez, P., Beiras, R., 2007. Contrasting complexing capacity of dissolved organic matter produced during the onset, development and decay of a simulated bloom of the marine diatom *Skeletonema costatum*. Mar. Chem. 103 (1–2), 61–75.
Maldonado, M.T., Hughes, M.P., Rue, E.L., Wells, M.L., 2002. The effect of Fe and Cu on growth and domoic acid production by Pseudo-nitzschia multiseries and Pseudo-nitzschia australis. Limnol. Oceanogr. 47 (2), 515–526.
Maldonado, M.T., et al., 2006. Copper-dependent iron transport in coastal and oceanic diatoms. Limnol. Oceanogr. 51 (4), 1729–1743.
Martin, J.H., Fitzwater, S.E., 1988. Iron-deficiency limits phytoplankton growth in the Northeast Pacific subarctic. Nature 331 (6154), 341–343.
McAlister, J.A., 2015. Biogeochemistry of Dissolved Gallium and Lead Isotopes in the Northeast Pacific and Western Arctic Oceans. University of British Columbia.
Measures, C.I., Landing, W.M., Brown, M.T., Buck, C.S., 2008. A commercially available rosette system for trace metal-clean sampling. Limnol. Oceanogr. 6, 384–394.
Miller, L.A., Bruland, K.W., 1997. Competitive equilibration techniques for determining transition metal speciation in natural waters: evaluation using model data. Anal. Chim. Acta 343 (3), 161–181.
Misumi, K., et al., 2013. Humic substances may control dissolved iron distributions in the global ocean: implications from numerical simulations. Glob. Biogeochem. Cycles 27 (2), 450–462.
Moffett, J.W., Dupont, C., 2007. Cu complexation by organic ligands in the sub-arctic NW Pacific and Bering Sea. Deep-Sea Res. Part I 54 (4), 586–595.
Moingt, M., Bressac, M., Belanger, D., Amyot, M., 2010. Role of ultra-violet radiation, mercury and copper on the stability of dissolved glutathione in natural and artificial freshwater and saltwater. Chemosphere 80 (11), 1314–1320.
Moore, C.M., et al., 2013. Processes and patterns of oceanic nutrient limitation. Nat. Geosci. 6 (9), 701–710.
Muller, F.L.L., Batchelli, S., 2013. Copper binding by terrestrial versus marine organic ligands in the coastal plume of River Thurso, North Scotland. Estuar. Coast. Shelf Sci. 133, 137–146.
Nishioka, J., Takeda, S., Wong, C.S., Johnson, W.K., 2001. Size-fractionated iron concentrations in the northeast Pacific Ocean: distribution of soluble and small colloidal iron. Mar. Chem. 74 (2), 157–179.
Omanovic, D., Gamier, C., Pizeta, I., 2015. ProMCC: an all-in-one tool for trace metal complexation studies. Mar. Chem. 173, 25–39.
Paulmier, A., Ruiz-Pino, D., 2009. Oxygen minimum zones (OMZs) in the modern ocean. Prog. Oceanogr. 80 (3–4), 113–128.
Peers, G., Price, N.M., 2006. Copper-containing plastocyanin used for electron transport by an oceanic diatom. Nature 441 (7091), 341–344.
Peers, G., Quesnel, S.A., Price, N.M., 2005. Copper requirements for iron acquisition and growth of coastal and oceanic diatoms. Limnol. Oceanogr. 50 (4), 1149–1158.
Posacka, A.M., et al., 2017. Dissolved copper (dCu) biogeochemical cycling in the subarctic Northeast Pacific and a call for improving methodologies. Mar. Chem. 196, 47–61.
Rivier, A., et al., 2012. Observed vs. predicted variability in non-algal suspended particulate matter concentration in the English Channel in relation to tides and waves. Geo-Mar. Lett. 32 (2), 139–151.
Rogan, N., et al., 2016. Volcanic ash as an oceanic iron source and sink. Geophys. Res. Lett. 43 (6), 2732–2740.
Romera-Castillo, C., Sarmento, H., Alvarez-Salgado, X.A., Gasol, J.M., Marrase, C., 2011. Net production and consumption of fluorescent colored dissolved organic matter by natural bacterial assemblages growing on marine phytoplankton exudates. Appl.

Environ. Microbiol. 77 (21), 7490–7498.
Rue, E., Bruland, K., 2001. Domoic acid binds iron and copper: a possible role for the toxin produced by the marine diatom Pseudo-nitzschia. Mar. Chem. 76 (1–2), 127–134.
Ruggiero, P., Interesse, F.S., Sciacovelli, O., 1979. [1H] and [13C]NMR studies on the importance of aromatic structures in fulvic and humic acids. Geochim. Cosmochim. Acta 43 (11), 1771–1775.
Ruzic, I., 1982. Theoretical aspects of the direct titration of natural-waters and its information yield for trace-metal speciation. Anal. Chim. Acta 140 (1), 99–113.
Sander, S.G., Koschinsky, A., Massoth, G., Stott, M., Hunter, K.A., 2007. Organic complexation of copper in deep-sea hydrothermal vent systems. Environ. Chem. 4 (2), 81–89.
Schallenberg, C., Davidson, A.B., Simpson, K.G., Miller, L.A., Cullen, J.T., 2015. Iron(II) variability in the northeast subarctic Pacific Ocean. Mar. Chem. 177, 33–44.
Schleicher, N., et al., 2010. Anthropogenic versus geogenic contribution to total suspended atmospheric particulate matter and its variations during a two-year sampling period in Beijing, China. J. Environ. Monit. 12 (2), 434–441.
Schuback, N., Schallenberg, C., Duckham, C., Maldonado, M.T., Tortell, P.D., 2015. Interacting effects of light and Iron availability on the coupling of photosynthetic electron transport and CO_2-assimilation in marine phytoplankton. PLoS One 10 (7).
Semeniuk, D.M., 2014. Copper Nutrition and Transport Mechanisms in Plankton Communities in the Northeast Pacific Ocean (PhD Thesis). University of British Columbia.
Semeniuk, D.M., et al., 2009. Plankton copper requirements and uptake in the subarctic Northeast Pacific Ocean. Deep-Sea Res. Part I 56 (7), 1130–1142.
Semeniuk, D.M., Bundy, R.M., Payne, C.D., Barbeau, K.A., Maldonado, M.T., 2015. Acquisition of organically complexed copper by marine phytoplankton and bacteria in the northeast subarctic Pacific Ocean. Mar. Chem. 173, 222–233.
Semeniuk, D.M., et al., 2016a. Using 67Cu to study the biogeochemical cycling of copper in the northeast subarctic Pacific Ocean. Front. Mar. Sci. (78), 3.
Semeniuk, D.M., et al., 2016b. Iron-copper interactions in iron-limited phytoplankton in the northeast subarctic Pacific Ocean. Limnol. Oceanogr. 61 (1), 279–297.
Shimotori, K., Omori, Y., Hama, T., 2009. Bacterial production of marine humic-like fluorescent dissolved organic matter and its biogeochemical importance. Aquat. Microb. Ecol. 58 (1), 55–66.
Sieburth, J.N., et al., 1987. The first methane-oxidizing bacterium from the upper mixing layer of the deep ocean: *Methylomonas pelagica* sp. nov. Curr. Microbiol. 14 (5), 285–293.
Smith, K., Costello, A., Lidstrom, M., 1997. Methane and trichloroethane oxidation by an estuarine methanotroph, *Methylobacter* ap. strain BB5.1. Appl. Environ. Microbiol. 63 (11), 4617–4620.
Sohn, M., Weese, D., 1986. 13C NMR spectra and Cu(II) formation constants for humic acids from fluvial, estuarine and marine sediments. Mar. Chem. 20 (1), 61–72.
Swarr, G.J., Kading, T., Lamborg, C.H., Hammerschmidt, C.R., Bowman, K.L., 2016. Dissolved low-molecular weight thiol concentrations from the US GEOTRACES North Atlantic Ocean zonal transect. Deep-Sea Res. Part I 116, 77–87.
Tang, D.G., Hung, C.C., Warnken, K.W., Santschi, P.H., 2000. The distribution of biogenic thiols in surface waters of Galveston Bay. Limnol. Oceanogr. 45 (6), 1289–1297.
Tsunogai, S., Sase, T., 1969. Formation of iodide-iodine in ocean. Deep-Sea Res. 16 (5), 489.
Ueno, H., Yasuda, I., 2003. Intermediate water circulation in the North Pacific subarctic and northern subtropical regions. J. Geophys. Res. 108 (C11).
Vance, D., et al., 2008. The copper isotope geochemistry of rivers and the oceans. Earth Planet. Sci. Lett. 274 (1–2), 204–213.
Walsh, M.J., Ahner, B.A., 2013. Determination of stability constants of Cu(I), Cd(II) & Zn (II) complexes with thiols using fluorescent probes. J. Inorg. Biochem. 128, 112–123.
Walsh, M.J., Goodnow, S.D., Vezeau, G.E., Richter, L.V., Ahner, B.A., 2015. Cysteine enhances bioavailability of copper to marine phytoplankton. Environ. Sci. Technol. 49 (20), 12145–12152.
Wells, M.L., Trick, C.G., Cochlan, W.P., Hughes, M.P., Trainer, V.L., 2005. Domoic acid: the synergy of iron, copper, and the toxicity of diatoms. Limnol. Oceanogr. 50 (6), 1908–1917.
Whitby, H., van den Berg, C.M.G., 2015. Evidence for copper-binding humic substances in seawater. Mar. Chem. 173 (0), 282–290.
Whitby, H., Hollibaugh, J.T., van den Berg, C.M.G., 2017. Chemical speciation of copper in a salt marsh estuary and bioavailability to Thaumarchaeota. Front. Mar. Sci. (178), 4.
Wong, G.T.F., 1991. The marine geochemistry of iodine. Rev. Aquat. Sci. 4 (1), 45–73.
Wong, G.T.F., Piumsomboon, A.U., Dunstan, W.M., 2002. The transformation of iodate to iodide in marine phytoplankton cultures. Mar. Ecol. Prog. Ser. 237, 27–39.
Yamashita, Y., Jaffe, R., 2008. Characterizing the interactions between trace metals and dissolved organic matter using excitation-emission matrix and parallel factor analysis. Environ. Sci. Technol. 42 (19), 7374–7379.
Yamashita, Y., Tanoue, E., 2009. Basin scale distribution of chromophoric dissolved organic matter in the Pacific Ocean. Limnol. Oceanogr. 54 (2), 598–609.
Yang, R.J., van den Berg, C.M.G., 2009. Metal complexation by humic substances in seawater. Environ. Sci. Technol. 43 (19), 7192–7197.